J. Phycol. **49,** 950–966 (2013)

DOI: 10.1111/jpy.12104

A NEW POTENTIALLY TOXIC *AZADINIUM* SPECIES (DINOPHYCEAE) FROM THE MEDITERRANEAN SEA, *A. DEXTEROPORUM* SP. NOV.[1]

Isabella Percopo

Taxonomy and Identification of Marine Phytoplankton Service, Stazione Zoologica Anton Dohrn, Villa Comunale, Naples 80121, Italy

Raffaele Siano

IFREMER, Centre de Brest, DYNECO/Pelagos, ZI de la Pointe du Diable CS 170, Plouzané 29280, France

Rachele Rossi, Vittorio Soprano

Dipartimento di Chimica, Istituto Zooprofilattico Sperimentale del Mezzogiorno, Via Salute 2, Portici, Naples 80055, Italy

Diana Sarno

Taxonomy and Identification of Marine Phytoplankton Service, Stazione Zoologica Anton Dohrn, Villa Comunale, Naples 80121, Italy

and Adriana Zingone[2]

Ecology and Evolution of Plankton Laboratory, Stazione Zoologica Anton Dohrn, Villa Comunale, Naples 80121, Italy

A new photosynthetic planktonic marine dinoflagellate, *Azadinium dexteroporum* sp. nov., is described from the Gulf of Naples (South Tyrrhenian Sea, Mediterranean Sea). The plate formula of the species, Po, cp, X, 4′, 3a, 6″, 6C, 5S, 6‴ and 2⁗, is typical for this recently described genus. *Azadinium dexteroporum* is the smallest representative of the genus (8.5 μm average length, 6.2 μm average width) and shares the presence of a small antapical spine with the type species *A. spinosum* and with *A. polongum*. However, it differs from all other *Azadinium* species for the markedly asymmetrical Po plate and the position of the ventral pore, which is located at the right posterior end of the Po plate. Another peculiarity of *A. dexteroporum* is the pronounced concavity of the second intercalary plate (2a), which appears collapsed with respect to the other plates. Phylogenetic analyses based on the large subunit 28S rDNA (D1/D2) and the internal transcribed spacer (ITS rDNA) support the attribution of *A. dexteroporum* to the genus *Azadinium* and its separation from the other known species. LC/MS-TOF analysis shows that *Azadinium dexteroporum* produces azaspiracids in low amounts. Some of them have the same molecular weight as known compounds such as azaspiracid-3 and -7 and Compound 3 from *Amphidoma languida*, as well as similar fragmentation patterns in some cases. This is the first finding of a species producing azapiracids in the Mediterranean Sea.

***Key index words: Azadinium*; azaspiracid; dinoflagellate; LC/MS-TOF; LTER-MC; Mediterranean Sea; phylogeny; taxonomy**

***Abbreviations*: AIC, Akaike information criterion; AZP, azaspiracid poisoning; BF, bright field; DAPI, 4′-6′-diamidino-2-phenylindole; DIC, differential interference contrast; DSP, diarrhetic shellfish poisoning; ESI, Electrospray Ionization interface; FSW, filtered seawater; hLRTs, hierarchical likelihood ratio tests; ITS, Internal Transcribed Spacer; LC/MS-MS, Time of Flight Mass Spectrometer; LC, Liquid Chromatography; LTER-MC, Long-Term Ecological Research Station MareChiara; ML, maximum likelihood; PH, phase contrast; pi, parsimony informative; SDC, Serial Dilution Culture**

The genus *Azadinium* was erected with the description of the species *A. spinosum* Elbrächter & Tillmann (Tillmann et al. 2009), followed shortly by the discovery of three other related small thecate dinoflagellates, *A. obesum* Tillmann & Elbrächter (Tillmann et al. 2010), *A. poporum* Tillmann & Elbrächter (Tillmann et al. 2011), and *A. polongum* Tillmann (Tillmann et al. 2012b). All these species were isolated from the North Sea, whereas a slightly different taxon, designated as *A.* cf. *poporum*, was recorded in the Pacific Ocean (Potvin et al. 2011). The recent transfer to the genus of a fifth species, *A. caudatum*, formerly known as *Amphidoma caudata* (Nézan et al. 2012), has widened the geographic range of the genus also to the Mediterranean Sea, where this species has been reported from the

[1]Received 20 November 2012. Accepted 24 May 2013.
[2]Author for correspondence: e-mail: zingone@szn.it.
Editorial Responsibility: O. De Clerck (Associate Editor)

Tyrrhenian Sea (Rampi 1969, as *Oxytoxum margalefi* and *Oxytoxum tonolli*), including the Gulf of Naples (AZ and DS, unpublished data), and from the Spanish (Delgado and Fortuño 1991, Margalef 1995) and Adriatic Sea coasts (Viličić et al. 1995, Totti et al. 2000). In addition, the report of a still unidentified species (*A.* cf. *spinosum*) from Argentinian waters (Akselman and Negri 2012) indicates that *Azadinium* species could be widespread and go unnoticed due to the small size (<20 μm) of most of them. All described *Azadinium* species were analyzed from the morphological and molecular point of view, with the exception of *A.* cf. *spinosum* that was only observed at light and electron microscopy from field fixed samples.

The genus *Azadinium* belongs to the subclass Peridiniphycidae and its Kofoidian plate formula is Po, cp, X, 4′, 3a, 6″, 6C, 5?S, 6‴ and 2⁗. It has affinities with both the orders Peridiniales and Gonyaulacales. The plate configuration of the epitheca in *Azadinium* matches that of Peridiniales rather than Gonyaulacales, while the number of precingular (6) and postcingular (6) plates, matches that of the Gonyaulacales, since Peridiniales generally have seven precingular and five postcingular plates. The configuration of the hypotheca, with a large posterior sulcal plate and two unequal antapical plates, also matches that of the Gonyaulacales, which, however, have a very distinct epithecal configuration. A recent phylogenetic study (Tillmann et al. 2012a) has supported the affiliation of the genus *Azadinium* to the family Amphidomataceae, formerly only including the genus *Amphidoma*. The latter genus shares the hypothecal plate pattern with *Azadinium*, but has six apical plates and lacks intercalary plates. Whether the Amphidomataceae are part of the Peridiniales or rather represent a distinct order still remains to be understood (Tillmann et al. 2012a).

The genus *Azadinium* owes its name to azaspiracids, which comprise a group of marine lipophilic biotoxins implicated in incidents of shellfish poisoning in humans, particularly in northern Europe. The first known AZP occurred in the Netherlands in 1995 after consumption of mussels (*Mytilus edulis*) cultivated on the west coast of Ireland (McMahon and Silke 1996). Probably AZP has often been confused with the DSP due to similar symptoms, including chills, headaches, diarrhea, nausea, vomiting, and stomach cramps. For several years, the heterotrophic peridinioid *Protoperidinium crassipes* (Kofoid) Balech has been the main suspected candidate for the production of AZA toxins (James et al. 2003), but the discovery of *A. spinosum* suggested that *P. crassipes* could have accumulated AZA toxins by grazing the actual culprit (Krock et al. 2009). Since the original AZP event, four additional events have occurred due to contaminated Irish mussels, in Ireland, Italy, France and United Kingdom, and 32 analogs of AZA have been identified in shellfish of many other coastal regions of Europe, Morocco, Chile, and Japan (Braña Magdalena et al. 2003, Taleb et al. 2006, Amzil et al. 2008, Ueoka et al. 2009, Alvarez et al. 2010, Furey et al. 2010). Of these, only AZA-1, -2 and -3 have been found in seawater samples (Furey et al. 2003) and the first two compounds in the species *Azadinium spinosum* (Tillmann et al. 2009), whereas the remainders are considered as transformation products within shellfish. All the other *Azadinium* species had not shown the presence of AZA toxins until the recent discovery of a distinct group of four azaspiracids of unknown toxicity in *A. poporum*, *A.* cf. *poporum,* and *Amphidoma languida* (Krock et al. 2012).

In October 2009, an unknown species of *Azadinium* was noticed for the first time in LM and SEM observations of fixed material from the Gulf of Naples (Mediterranean Sea), while a strain of the same species was successfully isolated 7 months after. Here, we report the morphological and molecular information of this specimen, which we described as a new species.

MATERIALS AND METHODS

Isolation and cultivation. The culture of a strain of *Azadinium dexteroporum* was obtained from a SDC experiment performed using a water sample collected on May 11, 2010 in surface waters at the LTER-MC, in the Gulf of Naples (Ribera d'Alcalà et al. 2004). SDCs were established in 24-well tissue culture plates (DB Falcon™, San Jose, CA, USA) filled with 1 mL of K/10 medium (Keller et al. 1987). Five replicates of five 1:10 dilution steps (from 1 mL to 0.1 μL) of the original sample were set up, following the method described in Andersen and Throndsen (2003) modified by Siano et al. (2009). Plates were kept at 20°C under an irradiance of 70–80 μmol photons $\cdot$ $m^{-2} \cdot s^{-1}$ and a 12:12 light:dark regime. Growth was checked every week. The presence of *A. dexteroporum* was noticed in one of the mixed cultures, from which the unialgal culture was established through further dilutions. The culture was maintained in K/10 medium at the same light and temperature conditions of the SDC plate. In addition, attempts were made to grow the strain of *A. dexteroporum* at three other temperature values (12, 15 and 18°C) and in full K medium.

Microscopy. Light microscopy (LM) observations and measurements of live culture material were carried out using a Zeiss Axiophot and Axiovert 200 light microscopes (Carl Zeiss, Oberkochen, Germany) equipped with Nomarski DIC, PH and BF optics. Cell length and width were measured using fixed cells (1% formaldehyde final concentration) and information on the shape and position of the nucleus was obtained by fixing cells with 1% formaldehyde and then staining them with DAPI (0.1 μg $\cdot$ mL^{-1}). Pictures were taken with a Zeiss Axiocam digital camera (Carl Zeiss).

For scanning electron microscopy (SEM) observations, samples were fixed with formaldehyde at 1% final concentration, placed on nuclepore 3 μm size-pore (Nuclepore, Pleasanton, CA, USA) polycarbonate filters, rinsed with distilled water, dehydrated in an ethanol series (25, 50, 75, 95, and 100%), and critical-point-dried. The filters were mounted on stubs, sputter-coated with gold-palladium and observed with a JEOL JSM-6500F SEM (JEOL-USA Inc., Peabody, MA, USA). SEM photographs were used to measure episome and hyposome length and width and other morphological structures not distinguishable at LM.

For transmission electron microscopy (TEM) observations, cells were concentrated by gentle centrifugation (800 rpm for 7 min), fixed with 1% (v:v) glutaraldehyde for 2 h at room temperature, rinsed with FSW, and post-fixed with 1% (v:v) osmium tetroxide for 1 h at room temperature. After two rinses with FSW, the sample was dehydrated in an ethanol series (25, 50, 75, 95, and 100%), transferred to propylene oxide, and embedded in Epon resin (v:v, 1:1). After polymerization at 70°C for 24 h, thin sections were obtained using a Leica Ultracut UCT (Leica Microsystems, Wetzlar, Germany), stained with uranyl acetate and lead citrate, and examined with a LEO 912AB (LEO, Carl Zeiss).

DNA extraction. Cells collected during the exponential growth phase were filtered on a 0.8 μm pore size Isopore membrane filter (Millipore, Schwalbach, Germany), and DNA was extracted using the CTAB procedure (Doyle and Doyle 1990). Two independent DNA extractions, followed by amplification and sequencing, were performed.

PCR and sequencing. Extracted DNA was subjected to polymerase chain reaction (PCR) for the amplification of the hypervariable (D1/D2) 28S ribosomal DNA region using the primers DIR (forward: 5′-ACC CGC TGA ATT TAA GCA TA 3′) and DIR-3Ca (reverse: 5′-ACG AAC GAT TTG CAG GTC AG-3′) (White et al. 1990), and for ITS using the primers ITSa (5′-CCA AGC TTC TAG ATC GTA ACA AGG (ACT)TC CGT AGG T-3′) and ITSb (5′-CCT GCA GTC GAC A(GT)A TGC TTA A(AG)T TCA GC(AG) GG-3′) (Orsini et al. 2002).

PCR was carried out in a PTC-200 Peltier Thermal Cycler (MJ Research, San Francisco, CA, USA). For the 28S rDNA amplification, the reaction mix was subjected to an initial denaturation at a temperature of 94°C for 5 min, followed by 34 cycles of denaturation at 94°C for 1 min, at 55°C for 1 min and 40 s and a final step at 72°C for 5 min. For ITS, an initial denaturation was performed at a temperature of 94°C for 50 s, followed by annealing at 60°C for 40 s and elongation at 72°C for 1 min; then 29 cycles of denaturation at 94°C for 45 s, at 50°C for 45 s and elongation at 72°C for 1 min. A final extension step was carried out for 5 min. The amplified fragments were purified using a QIAquick PCR purification kit (Qiagen Genomics, Bothell, WA, USA) following the manufacturer's instructions. Sequences were obtained from the PCR products with the BigDye Terminator Cycle Sequencing technology (Applied Biosystems, Forster City, CA, USA) and purified in automation using a robotic station "Biomek FX" (Beckman Coulter, Fullerton, CA, USA). Products were analyzed on an Automated Capillary Electrophoresis Sequencer "3730 DNA Analyzer" (Applied Biosystems).

Chromatograms of the sequences obtained were then analyzed by eye to check for the presence of double picks and base ambiguities.

Phylogenetic analysis. A dataset of 32 sequences was compiled with all available Amphidomataceae sequences and a systematically representative set of dinophytes was built for each marker (ITS, 28S) following the Table S2 from Tillmann et al. (2012b), and updating the taxonomic status of *Woloszynskia cincta* to *Biecheleria cincta* (Siano, Montresor & Zingone) Siano (Balzano et al. 2012). Sequences from the dataset and our *Azadinium* sequence were assembled using the BioEdit v. 4.8.5 computer package (Hall 1999) and aligned with the multiple sequences alignment program MUSCLE v. 3.7 (Edgar 2004) with the default settings. The alignments of the partial LSU and ITS were refined by eye and then concatenated. The resulting alignment is available as fasta file upon request. Phylogenetic analyses were carried out using ML and Bayesian approaches.

The software jModeltest v7.3 (Posada and Crandall 1998) was used to determine the best-suited nucleotide substitution model for the alignment. General Time Reversible model (GTR+C) was the first model as deduced by the hLRTs, AIC1, AIC2 and Bayesian Information Criterion (BIC) tests implemented in jModeltest (Table S1 in the Supporting Information). The dinoflagellate *Noctiluca scintillans* was selected as outgroup for all phylogenetic analyses. ML tree was constructed in MEGA 5.05 (Tamura et al. 2011). The robustness of tree topology was tested using bootstrap with 5,000 replications. Bayesian analyses were performed with TOPALI v.2.5 (Milne et al. 2008) using the best-fitting substitution model (GTR + G) and the random-addition-sequence method with 10 replicates. For each marker, 2 parallel runs with 1,000,000 generations, with a sample frequency of 10 and a burn-in of 25% were used. The calculation of the pairwise genetic distance was conducted using Mega version 5.0 (Tamura et al. 2011). All positions containing gaps and missing data were eliminated.

Toxin extraction. For azaspiracid analysis, two cultures of the strain of *A. dexteroporum* were grown in 1 L Erlenmeyer flasks at the same conditions as above with K and K/10 media, respectively. After 3 weeks, the cultures were centrifuged at 3,928*g* for 20 min. The pellet was sonicated for 10 min, resuspended in 1 mL of MeOH/W (8:2), vortexed for 1 min, and centrifuged at 1,500*g* for 5 min. The clear supernatant was transferred into a glass test tube without disturbing the pellet. The pellet was resuspended in 0.5 mL of MeOH/W (8:2), vortexed for 3 min, sonicated for 10 min, and centrifuged at 1,500*g* for 5 min. The new supernatant was collected and the pellet was submitted again to the extraction procedure. Then the pooled supernatants were evaporated and the residue was resuspended in 0.5 mL of MeOH/W (8:2). This sample extract was filtered on a 0.22 μm pore-size spin-filter (Millipore Ultrafree, Eschborn, Germany) and centrifuged at 11,769*g* for 5 min. The filtrate was transferred into an LC autosampler vial and 5 μL was injected for LC/MS/TOF analysis.

Determination of azaspiracids. Mass spectral experiments were performed on a MS-TOF (Agilent USA-Germany) coupled with a LC apparatus model 1100 (Agilent USA-Germany). The ESI was in positive ion mode. Phenomenex Luna C(8) 150 × 2.00 mm was used for chromatographic separation. Elution was accomplished with water (eluent A) and 95% acetonitrile/water (eluent B), both containing 50 mM formic acid and 2 mM ammonium formate. The flow rate was 0.2 mL · min^{-1}. The analyses were carried out by running a linear gradient elution, starting with 60% B for 6 min, followed by an increasing to 80% B in 0.5 min, 2 min hold at 80% B and decreasing to 60% B over 6 min (initial conditions). Water and acetonitrile were HPLC grade. The possible molecular formulas were accepted at a mass tolerance <5 ppm.

As compared to the triple quadrupole and q-trap LC/MS-MS used in other azaspiracid studies, the LC/MS-TOF used in this study does not perform a specific fragmentation, since it lacks a collision cell, but some fragments are still obtained in the ESI source. The spectrum obtained in LC/MS-TOF from the azaspiracid-1 (AZA-1) reference material (NRC CRM AZA-1, NRC, Canada) was analyzed as a first step of the study. The analytical standard of AZA-1 was injected at a concentration of 620 ng · mL^{-1}.

The LC/MS-TOF analysis worked in positive ion mode, with mass range set at *m/z* 300–1000 at a resolving power of 10,000. The conditions of the ESI source were as follows: drying gas (N_2) flow rate, 8 mL · min^{-1}; drying gas temperature, 350°C; nebulizer, 45 psig; capillary voltage, 4000 V; fragmentor 350 V; skimmer voltage, 60 V. All the acquisitions and data analysis were controlled by the Agilent LC/MS-TOF Software. A tuning mix (G1969-85001) was used for lock mass calibration.

Extracted ion chromatograms (EIC) were obtained for the 36 so far identified azaspiracid molecules by selecting their exact mass weight $(M+H)^+$. The exact masses (Table S2 in the Supporting Information) were calculated on the basis of the structural information on the molecules reported in Table 2 in Twiner et al. (2008) and of the molecular formulae in Krock et al. (2012).

RESULTS

Azadinium dexteroporum Percopo et Zingone **sp. nov.**

Photosynthetic thecate dinoflagellate. Ellipsoidal cells, 7.0–10.0 μm long and 5.0–8.0 μm wide. One lobed chloroplast extending into both epi- and hyposome, with one pyrenoid visible in the episome. Nucleus spherical, placed in the posterior part of the cell. Thecal tabulation: Po, cp, X, 4′, 3a, 6″, 6C, 5?S, 6‴ and 2⁗. Episome with a conspicuous apical pore complex. Hyposome asymmetric, smaller than the episome and bearing a small antapical spine on its right side, on the 2⁗ plate. Cingulum excavated and wide about one quarter of the cell length. Po asymmetrical, its right end extending posteriorly in the epitheca between plates 1′ and 4′. Ventral pore located at the posterior right end of the Po plate, surrounded by 1′ and 4′ plates. 1″ plate in contact with the 1a intercalary plate. Plate 2a four-sided and concave. Postcingular plates quadrangular, with 1‴ and 6‴ smaller than the others.

HOLOTYPE: Figure 2A, SEM stub n. 2211-5, deposited at the SZN Museum.

ISOTYPE: Formalin fixed sample strain SZN-B848, deposited at the SZN Museum.

TYPE LOCALITY: LTER-MareChiara, 40°48′ 50″ N; 14°15′ 0″ E, Gulf of Naples, Italy (South Tyrrhenian Sea, Mediterranean Sea).

HABITAT: Marine plankton.

ETYMOLOGY: The epithet refers to the position of the ventral pore with respect to 1′ plate.

Cell morphology. Cells are slightly elongated (length/width ratio = 1.4) and dorso-ventrally compressed (Figs. 1, A–I and 2, A–F), 7–10 μm in length (avg 8.5 μm, $n = 53$) and 5.0–8.0 μm in width (avg 6.2 μm, $n = 53$). The episome (3.2–4.4 μm in length and 5.0–6.2 μm in width) is about three times longer and slightly larger than the hyposome (1.1–1.8 μm in length and 4.6–5.0 μm in width) and is characterized by a prominent apical pore complex (APC; Figs. 1, A, F; and 2, A, B). The hyposome is slightly asymmetrical (Figs. 1, A, F, H; and 2A), with a small spine located in its posteriormost right side (Figs. 1, H, I and 2, A–F). The cingulum is deeply excavated and notably wide (1.8–2.4 μm), occupying ca one quarter of the cell length (Fig. 2, A–E). Cells have a single lobed chloroplast, at times limited to the episome (Fig. 1C) but generally extending into the whole protoplast (Fig. 1D), and a spherical nucleus located in the posterior part of the cell (Fig. 1B). One large pyrenoid is visible in the episome (Fig. 1, A, E–G). At times other prominent, rounded bodies are seen in the episome, which differ from pyrenoids for the absence of a clear starch shield around them (Fig. 1, F and G).

Azadinium dexteroporum generally swims at low velocity, without a preferential direction, sometimes with a zigzag pattern. This quiet swimming is often interrupted by sudden speedup accompanied by a change of direction.

The basic thecal plate arrangement (Fig. 3, A–F) is Po, cp, X, 4′, 3a, 6″, 6C, 5?S, 6‴ and 2⁗. The generally teardrop-shaped apical pore is positioned in the center of pore plate (Po) and connected through a finger-like protrusion to the small X plate (X), which posteriorly touches the first apical plate (1′). Po surrounds the cover plate (cp) with a raised proximal rim and is markedly asymmetrical on its ventral side, where it abuts the two sides of the X plate continuing to the right with a long protrusion, which runs between plates 1′ and 4′ (Fig. 4, A–E). A conspicuous ventral pore (vp), 0.25–0.35 μm in diameter, is placed at the end of this protrusion, surrounded by the ventral margins of plates 1′ and 4′ which join posterior to it. Po is delimited by the thickened rim of the four apical plates all along its posterior margin. The rims of 1′ and 4′ continue ventrally, bordering the vp (Fig. 4, A, C–E).

The four-sided (ortho pattern) 1′ plate is slightly asymmetrical anteriorly and has a narrow posterior end (Figs. 2A and 4C). Plates 2′ and 3′ are small and quite similar in size, whereas plate 4′ is slightly larger (Fig. 4B). The intercalary plates 1a and 3a are pentagonal and similar in size whereas the central 2a is four-sided and smaller (Fig. 4, A and B). This plate is concave and does not lie in the same plane of the surrounding ones, but is typically collapsed with respect to them (Fig. 4, A and B and 5B). The six precingular plates are similar in size, with the exception of the 6″ which is slightly narrower. 1″ plate has five sides and is in contact with four epithecal plates, in addition to the first cingular (C1) and sulcal anterior (Sa) plates: the intercalary plate (1a), the apical 1′, 2′, and the precingular 2″ (Fig. 4, A and B).

All postcingular plates have four sides and similar size with the exception of the 1‴ and the 6‴ which are the smallest ones (Fig. 4F). Of the two antapical plates, 2⁗ plate is much larger and bears a short and pointed antapical spine on its right side (Fig. 4, F, G). A variable number of small pores are present on 2⁗ plate around the antapical spine (Fig. 4F).

The cingulum is wide and descending, displaced by half its width. It is comprised of six plates of similar size. Narrow cingular lists are formed by the posterior margins of the precinglular plates and anterior margins of the postcingular plates (Fig. 4F). The sulcus is comprised of five main plates: Sa is longer than wide and broadly rectangular (Figs. 2A and 4G). It is the largest plate in the sulcus. The posterior sulcal plate (Sp) is as wide as long (Figs. 3A and 4G), with six sides which touch C6, 6‴, 2⁗, 1⁗,

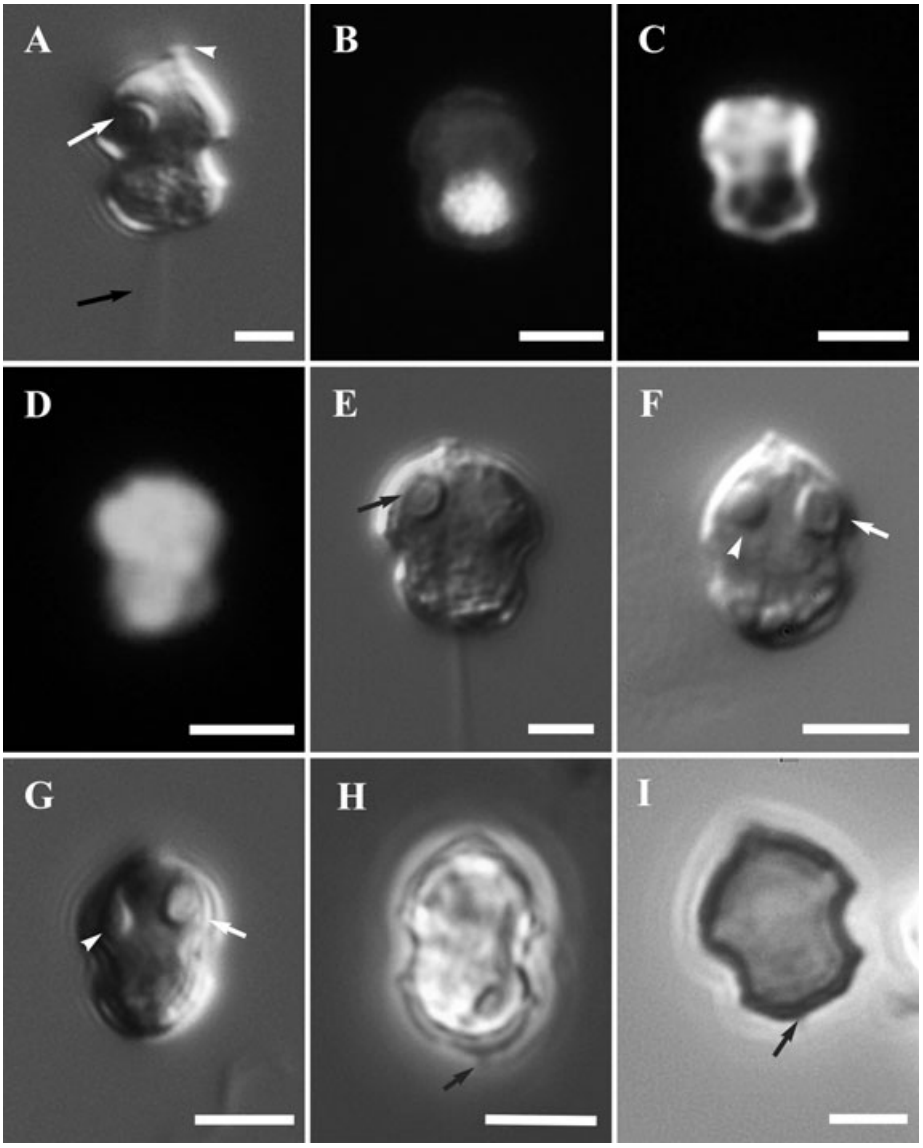

FIG. 1. (A–H) *Azadinium dexteroporum*, LM graphs. Scale bars: (A–D, F–H) = 5 μm, (E, I) = 2 μm. (A) live cell in ventral view. Note the apical pore complex (arrowhead), the pyrenoid (white arrow) and the flagella emerging from the sulcus (black arrow), (B) DAPI staining of the nucleus, (C) chlorophyll fluorescence: the chloroplast is mainly visible in the episome, (D) chlorophyll fluorescence: the chloroplast in whole cell, (E) live cell with one pyrenoid in the episome (arrow), (F) live cell with pyrenoid (white arrow) and accumulation body (arrowhead). Note the prominent apical pore complex (black arrow), (G) live cell with pyrenoid (arrow) and accumulation body (arrowhead), (H) cell from natural sample in dorsal view. Note the antapical spine (arrow), (I) specimen from natural sample, empty theca. Note the antapical spine (arrow).

1‴ and Ss. The left sulcal plate (Ss) is short and widely S-shaped and is in contact with C6, Sp, 1‴, C1, Sa, Sm and Sd plates. The right sulcal plate (Sd) is small and touches the C6, Ss and Sm plates. The median sulcal plate (Sm) is small and contacts C6, Sd, Ss and Sa plates (Fig. 4, H and I). A thin anterior accessory sulcal plate is visible in some cases anterior to Sm and Sd (Fig. 4, H and I).

Thecal plates are smooth and most of them show one or a few trichocyst pores in quite fixed positions. For example, two (at times three) close pores are always seen on 1′ plate (Fig. 4, C–E), while a group of pores are invariably seen in the middle of 1a and 3a (Fig. 4B). Almost all pre- and post-cingular plates have one or a few pores at one corner toward the cingulum (e.g., Figs. 2, B and E and 4F). Very few variations were observed in the theca of the cultured strain. A scanning image from natural material (Fig. 2F) also showed a consistent morphology. In some specimens the antapical spine was thickened at its tip (Fig. 5A), while at times the apical plates 2′ and 3′ were not separated, resulting in three instead of four apical plates (Fig. 5B).

Under TEM a big rounded nucleus with condensed chromosomes is visible in the posterior part of the cell (Fig. 6, A and B). One lobed peripheral

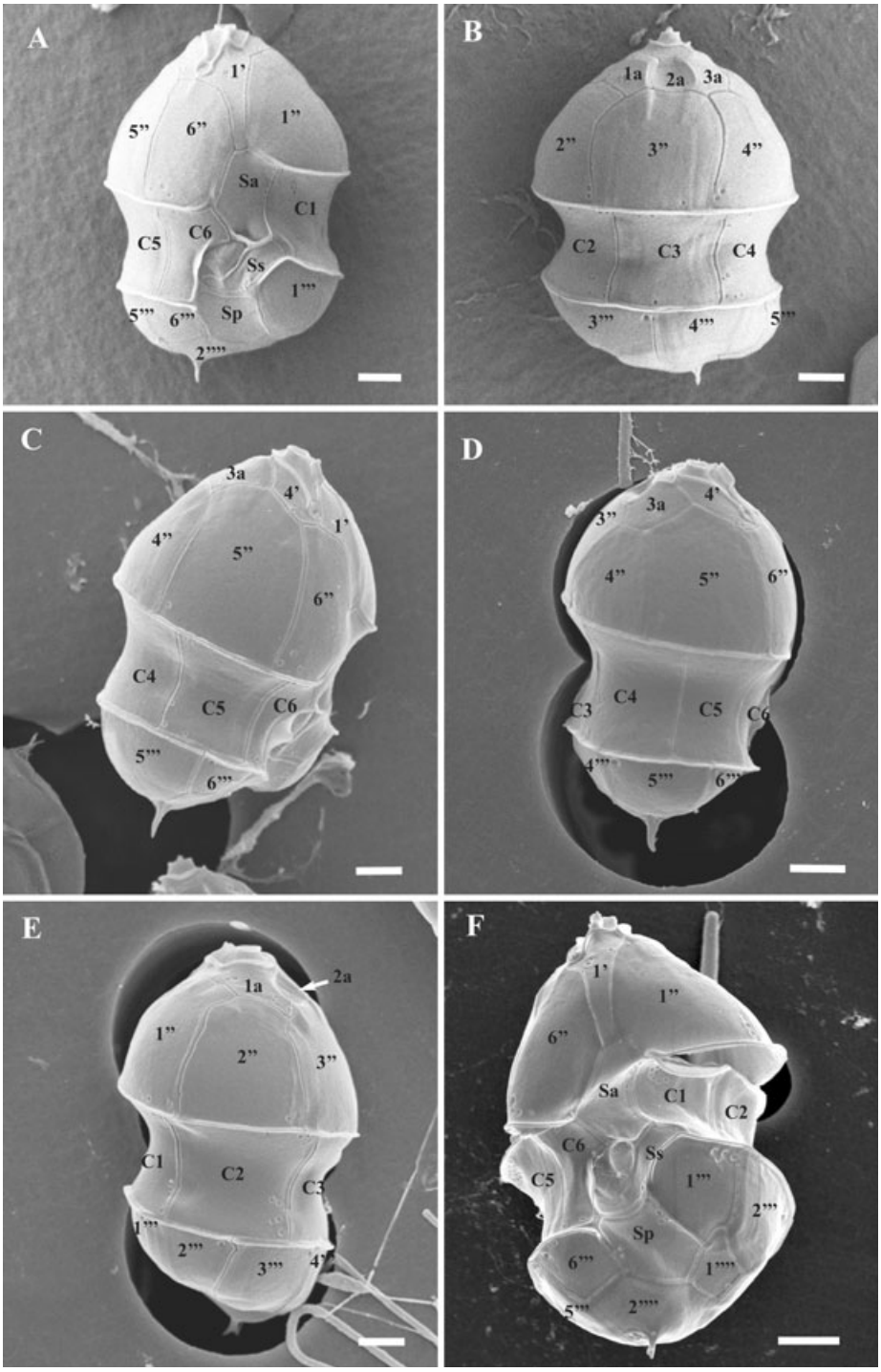

FIG. 2. (A–F) *Azadinium dexteroporum*, SEM graphs; scale bars = 1 μm. (A) ventral view, (B) dorsal view, (C) right antero-lateral view, (D) right lateral view, (E) left lateral view, (F) ventral view, cell from natural sample.

chloroplast is present (Fig. 6, B and C). A large pyrenoid with starch sheath is located in the anterior part of the cell. It consists of a spherical/ovoid granular structure connected to the terminal part of the chloroplast by a projection (Fig. 6, A–D). Several accumulation/lipid bodies with unidentified content are present in whole cell (Fig. 6, A–E). Several trichocysts are observed which appear as irregular quadrangular or polygonal bodies in transversal sections (Fig. 6, D and F). A large fibrous body is almost always visible associated with the anterior part of the nucleus. It contains fine fibrous material of unknown composition and function (Fig. 6, C and G).

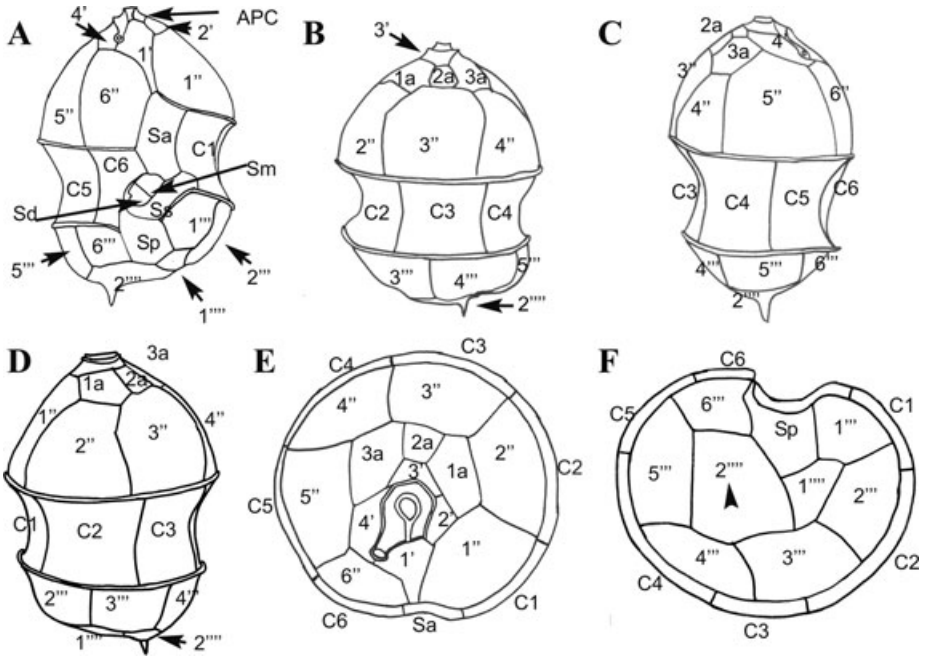

FIG. 3. (A–F) *Azadinium dexteroporum*. Schematic drawings with plate tabulation. (A) ventral view, (B) dorsal view, (C) right side, (D) left side, (E) apical view, (F) antapical view (arrowhead: antapical spine). APC, apical pore complex; Sa, anterior sulcal plate; Sd, right sulcal plate; Sm, median sulcal plate; Sp, posterior sulcal plate; Ss, left sulcal plates.

Additional information. In the laboratory, best growth was obtained with K/10 medium, while the growth was very slow in full K medium. The culture did not grow at temperature values lower than 18°C.

Molecular results. The total length of the rDNA alignment for the 33 taxa was 1,272 bases, with 582 sites being pi (45%). The ITS region covered 711 bases with 366 pi sites (51%) and the first two domains of the LSU covered 561 bases with 233 pi sites (41%). Tree topologies inferred from Bayesian and ML approaches were largely congruent. The best scoring ML tree is shown in Figure 7.

Although the basal nodes were not all resolved with high support, taxonomic units such as the Gymnodiniales 1, Gymnodiniales 2, Prorocentrales, and Amphidomataceae were distinguished. Within the Amphidomataceae, *Amphidoma languida* was the most basal taxon. Within the genus *Azadinium*, the species *A. spinosum*, *A. poporum*, *A. polongum*, *A. caudatum* var. *margalefii*, *A. caudatum* var. *caudatum* and the new species *A. dexteroporum* formed a clear and highly supported clade, whereas the clade formed by *A. obesum* and *A.* cf. *poporum* was highly supported only with the Bayesian analysis. The concatenated tree inferred from partial LSU and ITS regions (Fig. 7) showed *A. dexteroporum* clearly distinct and basal to all the *Azadinium* species, with a high support value.

The genetic distance based on the whole ITS region also confirmed the separation of the new species from all the other Amphidomataceae (Table S3 in the Supporting Information). The distance varied between 0.129 and 0.270, which were the distances of *A. dexteroporum* from *A. obesum* and the recently described species *A. polongum*, respectively.

Toxin pattern. Of the 36 azaspiracid molecules so far identified, only the $(M+H)^+$ ions of MW 828.48980, MW 858.50036, and of MW 830.50545, showed defined peaks in the chromatogram obtained from the analysis of the *A. dexteroporum* sample extract. The EIC and the High Resolution Mass Spectrum (HRMS) with the fragmentation patterns of the three molecules, along with the ones of AZA-1 from the standard material, are shown in Figures 8 and 9, while their possible molecular formulas are reported in Table 1.

The AZA-1 molecule from the reference material eluted at 6.9 min (Fig. 9A). Its spectrum (Fig. 9C) showed the formation of a predominant $(M+H)^+$ ion, its two subsequent water losses and the characteristic A-ring fragment at *m/z* 672, C_{19}-C_{20} fragment at *m/z* 462 and E-ring fragment at *m/z* 362. All three of these fragments showed one water loss.

The spectrum of the molecule of MW 858 (Fig. 9, B and D) showed the same pattern as AZA-1, with the formation of the known ions at *m/z* 858 $(M+H)^+$, *m/z* 840 $(M+H-H_2O)^+$, *m/z* 822 $(M+H-2H_2O)^+$, and at *m/z* 672 $(M+H-H_2O-C_9H_{12}O_2)^+$. The fragment at *m/z* 672.4 has been considered as a clear diagnostic signal, allowing to distinguish AZA-7 from its isomers AZA-8, -9 and -10 (James et al. 2003), while the fragments at *m/z* 462 (C_{19}-C_{20} fragment) and *m/z* 362 (E- ring) would be distinctive for AZA-7 in comparison with the "Compound 1"

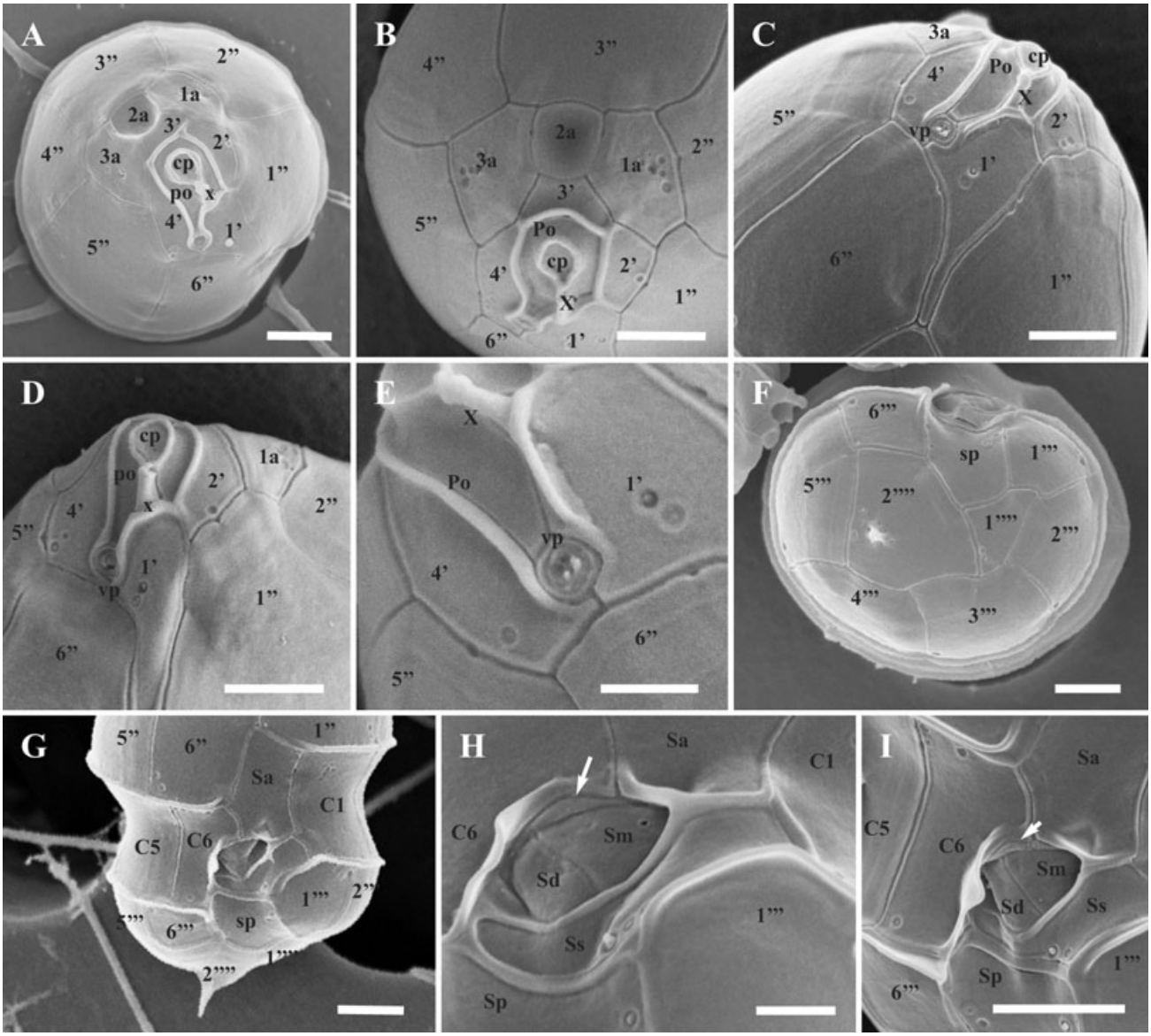

FIG. 4. (A–I) *Azadinium dexteroporum*, SEM graphs. Scale bars: (A–D, F, G, I) = 1 μm, (E, H) = 0.5 μm. (A) apical view, (B) detail of the epitheca, apical view, (C) detail of the epitheca, ventral view. Note the narrow 1′, (D, E) details of the apical pore complex. Note the ventral pore, (F) antapical view, (G) hypotheca in ventral view, (H, I) detail of sulcal plates. Note the small anterior accessory plate (arrow).

found in *A. poporum* (Krock et al. 2012). The latter has the same MW and formula as AZA-7 but a different structure and fragmentation pattern (Krock et al. 2012), with the A-ring fragment at m/z 658, the D-ring fragment at m/z 448 and the E-ring fragment at m/z 348. However, the spectrum of the molecule MW 858 from *A. dexteroporum* also showed the formation of the ion $(M+H\text{-}CO_2)^+$ at *m/z* 814 and its subsequent loss of water molecules at *m/z* 796 and 778, which are reported for "Compound 1" (Krock et al. 2012), suggesting that this molecule is a new isomer of AZA-7.

The molecule from *A. dexteroporum* eluting at 4.9 min (Fig. 10A) had the same MW 828 and fragmentation pattern as reported for AZA-3 (James et al. 2003). This consisted of the $(M+H)^+$ ion at *m/z* 828, the water loss $(M+H\text{-}H_2O)^+$ at *m/z* 810 and the typical A-ring fragmentation at *m/z* 658 (Fig. 9, A and B). However, due to the characteristics of the LCTOF system, it cannot be excluded that the latter fragment may derive from other molecules. Therefore, the identity of the molecule at MW 828 needs to be confirmed with further analyses. In addition, the chromatogram of the MW 828 molecule from *A. dexteroporum* showed three peaks at the retention time of 1, 7 and 9.5 min (Fig. 10A). While the first one was probably due to uncharacterized unbound impurities eluting with the solvent front, the other two contained molecules similar to azaspiracids. Yet the spectrum of the 7 min peak lacked the

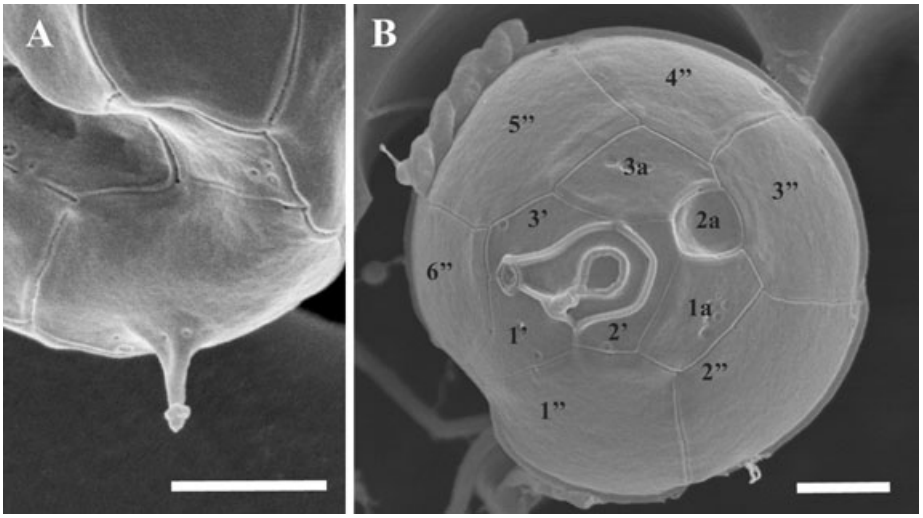

FIG. 5. (A–B) *Azadinium dexteroporum*, SEM graphs. Variations observed in cultured material; scale bars = 1 μm. (A) detail of the hypotheca, showing the spine with thickened tip, (B) unusual apical plate pattern, with three instead of four apical plates.

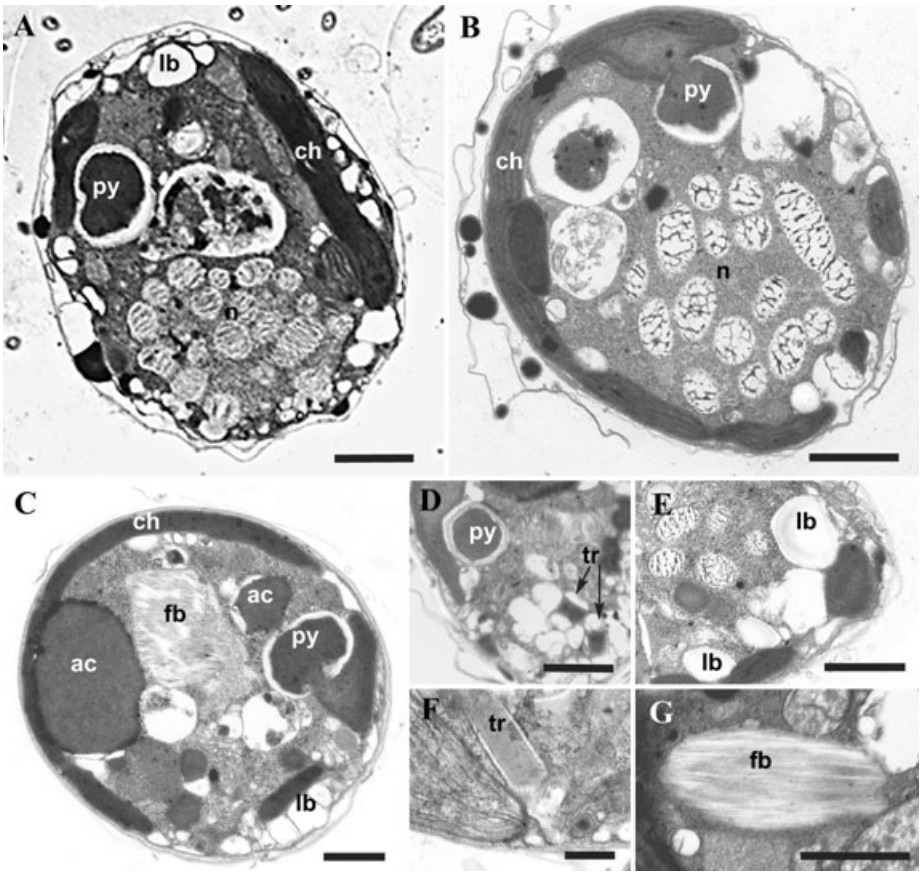

FIG. 6. (A–G) *Azadinium dexteroporum*, TEM graphs. Scale bars: (A–E, G) = 1 μm, (F) 0.2 μm, (A, C) cell sections showing the large nucleus (n), the pyrenoid (py) with the starch sheath, the chloroplast (ch), accumulation (ac) and lipid bodies (lb), and fibrous body (fb), (D) detail showing pyrenoid and transversal cuts of trichocysts (tr), (E) detail with lipid bodies, (F) longitudinal cut of a trichocyst, (G) fibrous body.

characteristic fragmentation of the A-ring while the one at 9.5 min did not show the typical water loss ions, thus leaving the identification of these molecules uncertain. The C_{19}-C_{20} and E-ring fragment were not detected, due to the low amount of these molecules and to the interference of the matrix.

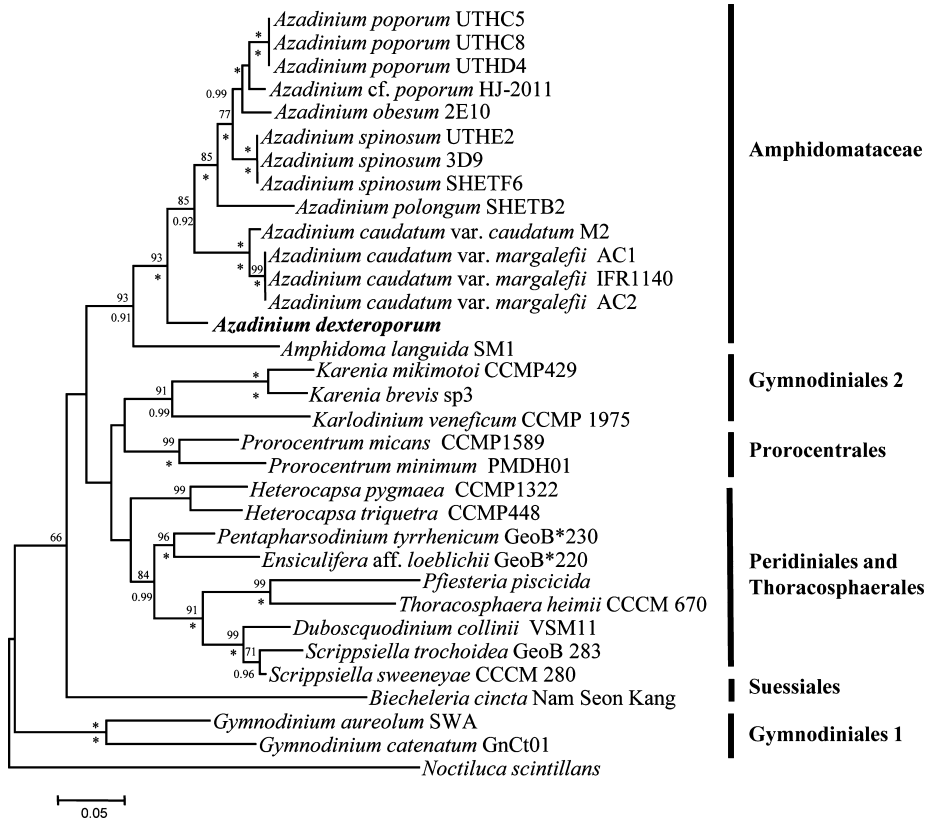

FIG. 7. Phylogenetic tree inferred from concatenated partial LSU (D1-D2) and ITS sequences based on maximum likelihood (ML) and Bayesian inference (BI). *Noctiluca scintillans* was used as outgroup. The new species is indicated in bold. Numbers on branches are statistical support values (above: ML bootstrap support values, <60 not shown; below: Bayesian posterior probabilities, <0.90 not shown; maximal support is indicated by an asterisk). Scale bar = number of nucleotide substitutions per site.

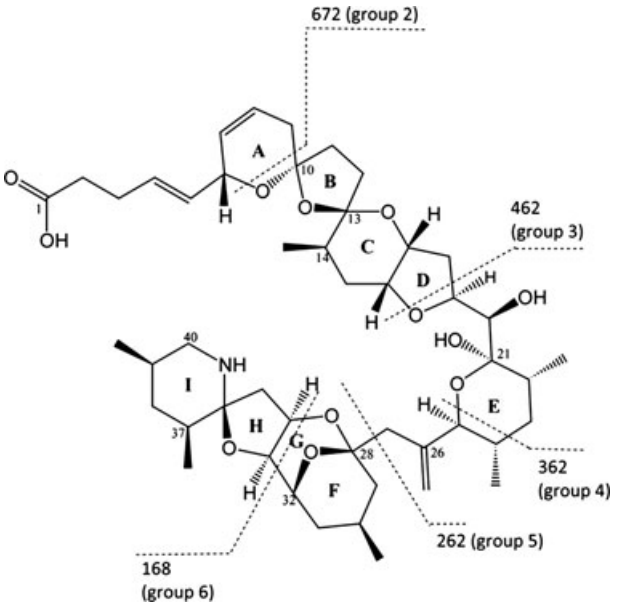

FIG. 8. Structure of azaspiracid 1 and CID cleavage sites (redrawn from Krock et al. 2012).

As for the third molecule from the *A. dexteroporum* extract (Fig. 10C), it showed the molecular ion at m/z 830, along with the formation of the water losses at *m/z* 812 and at *m/z* 794, but it lacked the characteristic A-ring fragmentation at *m/z* 686.4 seen in the Compound 3 from *A. languida* (Krock et al. 2012), which has the same MW. Finally, several other azaspiracid-like molecules were detected in the extract from *A. dexteroporum*, which deserve more detailed investigations.

Experiments of spike and recovery of known amounts of analyte into various samples of azaspiracid-free strains (the diatom *Leptocylindrus danicus* Cleve) indicated the detection limit of the method as a cell quota of about 0.01 fg per cell. The concentration of the different azaspiracid-like molecules in the cells was estimated by direct comparison with the AZA-1 standard, based on the high similarity among the different azaspiracid molecules. The amount of each AZA analog was low (Table 2), and varied considerably between the two subcultures, but the molecule MW 858 was always the most abundant (2.22–3.68 fg per cell).

DISCUSSION

Both molecular and morphological results presented in this study support the identification of the specimens found in the Mediterranean Sea as a new species of the genus *Azadinium*, here described

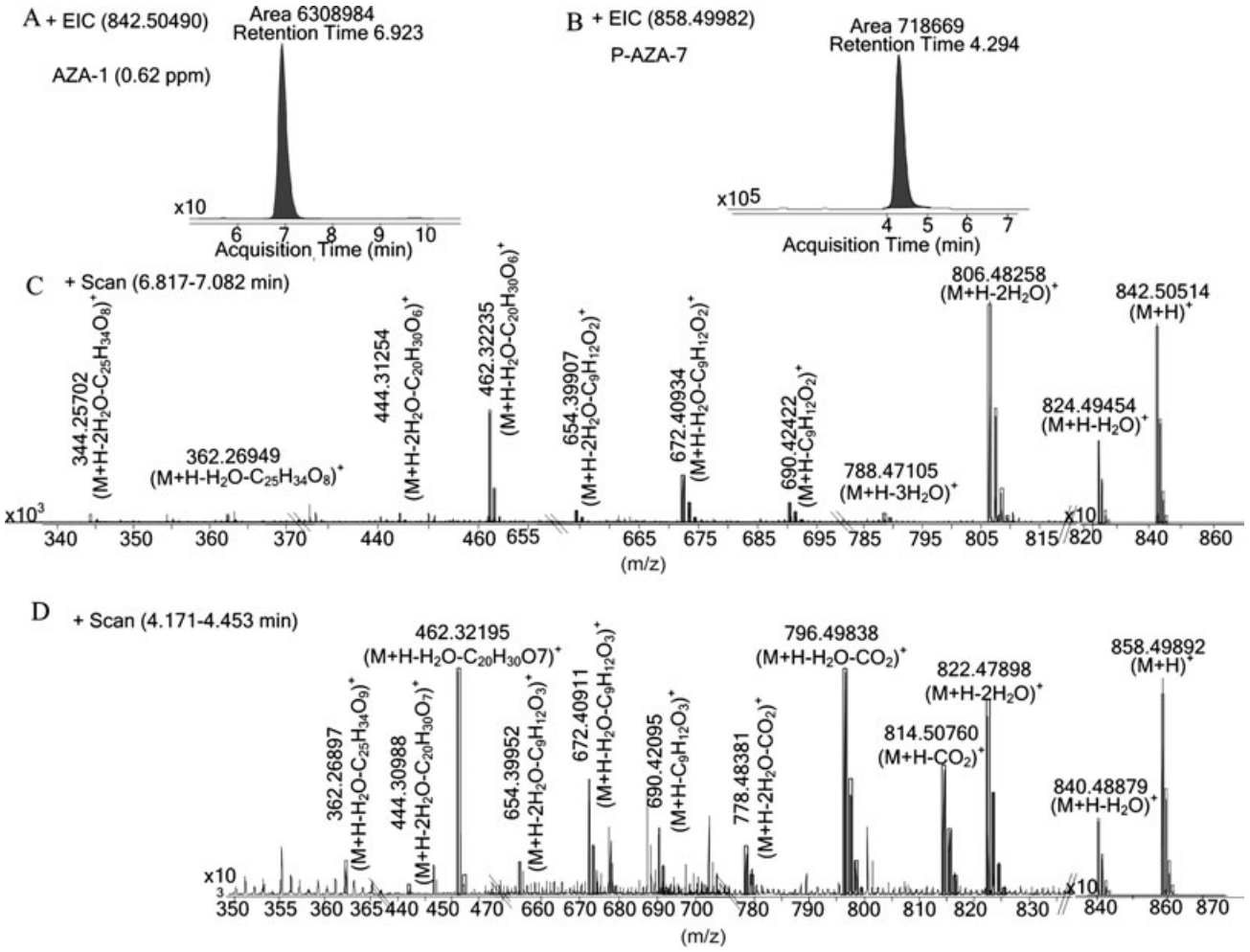

FIG. 9. (A–D) LC/MS-TOF characterization of azaspiracid 1 (AZA-1) from the reference material and molecule MW 858 (P-AZA-7) from the *Azadinium dexteroporum* culture extract. (A) Extracted Ion Chromatogram (EIC) of AZA-1, (B) EIC of molecule 858, (C) HRMS spectrum of AZA-1, (D) HRMS of molecule 858.

under the name *A. dexteroporum*. The thecal plate tabulation of *A. dexteroporum* perfectly fits into the genus *Azadinium* within the subclass Peridiniphycidae family Amphidomataceae (Tillmann et al. 2012a). The species has the same plate formula as all other *Azadinium* species, with which it shares the presence of a typical ventral pore, which is also seen in the sister genus *Amphidoma*. Other characteristics, such as the presence of an antapical spine and the production of azaspiracids, also support the attribution of the new species to *Azadinium*, although these features are not shared by all the species in the genus, nor are they unique to the genus.

The phylogenetic analyses clearly highlight the stability of the genus and, and along with the relatively high genetic distances of the ITS region, support the separation of *A. dexteroporum* from the other described species. Six species are now clearly distinguishable within the *Azadinium* genus (Tillmann et al. 2009, 2010, 2011, 2012b, Nézan et al. 2012). The position of *A. dexteroporum*, at the base of all the other species in the genus, and its wide genetic distance from *A. polongum*, are somewhat surprising as, at least at first sight, the morphology of the new species would place it closer to the smaller *Azadinium* and would better fit with *A. caudatum* as external to all the species originally described in the genus.

The main morphological features that allow the discrimination of *A. dexteroporum* from the other congeneric species are the marked asymmetry of the Po plate and the position of the ventral pore (vp) at its right posterior end, in touch with 1′ and 4′ plates. The position of the vp in *A. dexteroporum* is opposite to that observed in *A. poporum*, where it is located at the posterior left end of the Po plate, touching plate 1′ and 2′, but in that case the Po plate is more symmetrical. In the type species *A. spinosum* and in *A. obesum* and *A. polongum* the vp is located on the mid left margin of 1′ plate (Tillmann et al. 2009, 2011, 2012b). Therefore, *A. dexteroporum* is so far the only species, among those originally described as *Azadinium*, having the vp on

TABLE 1. Diagnostic ions of the molecules identified in the reference material (AZA-1) and in the cultured cells (putative AZA-3, molecule 858 and molecule 830).

AZA-1	**$(M+H)^+$**	**$(M+H-H_2O)^+$**	**$(M+H-2H_2O)^+$**	**$(M+H-3H_2O)^+$**	**$(M+H-C_9H_{12}O_2)^+$**	**$(M+H-H_2O-C_9H_{12}O_2)^+$**
Calculated MW	842.50490	824.49434	806.48377	788.47321	690.42117	672.41051
Effective MW	842.50514	824.49454	806.48258	788.47105	690.42422	672.40934
Δppm	−0.28	−0.24	1.48	2.73	−4.41	1.88
Chemical formula	$C_{47}H_{72}NO_{12}$	$C_{47}H_{70}NO_{11}$	$C_{47}H_{68}NO_{10}$	$C_{47}H_{66}NO_9$	$C_{38}H_{60}NO_{10}$	$C_{38}H_{58}NO_9$
(ctd.)	**$(M+H-2H_2O-C_9H_{12}O_2)^+$**	**$(M+H-H_2O-C_{20}H_{30}O_6)^+$**	**$(M+H-2H_2O-C_{20}H_{30}O_6)^+$**	**$(M+H-H_2O-C_{25}H_{34}O_8)^+$**	**$(M+H-2H_2O-C_{25}H_{34}O_8)^+$**	
Calculated MW	654.40004	462.32140	444.31084	362.26897	344.25841	
Effective MW	654.39907	462.32235	444.31254	362.26949	344.25702	
Δppm	1.49	−2.06	−3.84	−1.43	4.04	
Chemical formula	$C_{38}H_{56}NO_8$	$C_{27}H_{44}NO_5$	$C_{27}H_{42}NO_4$	$C_{22}H_{36}NO_3$	$C_{22}H_{34}NO_2$	
Putative AZA-3	**$(M+H)^+$**	**$(M+H-H_2O)^+$**	**$(M+H-2H_2O)^+$**	**$(M+H-H_2O-C_8H_8O_3)^+$**		
Calculated MW	828.48925	810.47869	792.46867	658.43134		
Effective MW	828.49117	810.48168	n.d.	658.42917		
Δppm	−2.31	−3.69	n.d.	3.31		
Chemical formula	$C_{46}H_{70}NO_{12}$	$C_{46}H_{68}NO_{11}$	$C_{46}H_{66}NO_{10}$	$C_{38}H_{60}NO_8$		
Molecule 858	**$(M+H)^+$**	**$(M+H-H_2O)^+$**	**$(M+H-2H_2O)^+$**	**$(M+H-C_9H_{12}O_3)^+$**	**$(M+H-H_2O-C_9H_{12}O_3)^+$**	**$(M+H-2H_2O-C_9H_{12}O_3)^+$**
Calculated MW	858.49982	840.48925	822.47869	690.42117	672.41061	654.40004
Effective MW	858.49892	840.48879	822.47898	690.42095	672.40911	654.39952
Δppm	1.05	0.55	−0.35	0.32	2.23	−0.80
Chemical formula	$C_{47}H_{72}NO_{13}$	$C_{47}H_{70}NO_{12}$	$C_{47}H_{68}NO_{11}$	$C_{38}H_{60}NO_{10}$	$C_{38}H_{58}NO_9$	$C_{38}H_{56}NO_8$
(ctd.)	**$(M+H-CO_2)^+$**	**$(M+H-H_2O-CO_2)^+$**	**$(M+H-2H_2O-CO_2)^+$**	**$(M+H-H_2O-C_{20}H_{30}O_7)^+$**	**$(M+H-2H_2O-C_{20}H_{30}O_7)^+$**	**$(M+H-H_2O-C_{25}H_{34}O_9)^+$**
Calculated MW	814.50999	796.49942	778.48886	462. 32140	444.31084	362.26897
Effective MW	814.50760	796.49838	778.48381	462.32195	444.30988	362.26855
Δppm	2.93	1.38	6.49	−1.19	2.14	1.17
Chemical formula	$C_{46}H_{72}NO_{11}$	$C_{46}H_{70}NO_{10}$	$C_{46}H_{68}NO_9$	$C_{27}H_{44}NO_5$	$C_{27}H_{42}NO_4$	$C_{22}H_{36}NO_3$
Molecule 830	**$(M+H)^+$**	**$(M+H-H_2O)^+$**	**$(M+H-2H_2O)^+$**	**$(M+H-H_2O-C_7H_{10}O_2)^+$**		
Calculated MW	830.50490	812.49434	794.48377	686.42082		
Effective MW	830.50590	812.49581	794.48699	n.d.		
Δppm	−1.20	−1.81	−4.05	n.d.		
Chemical formula	$C_{46}H_{72}NO_{12}$	$C_{47}H_{70}NO_{11}$	$C_{47}H_{68}NO_{10}$	$C_{39}H_{60}NO_9$		

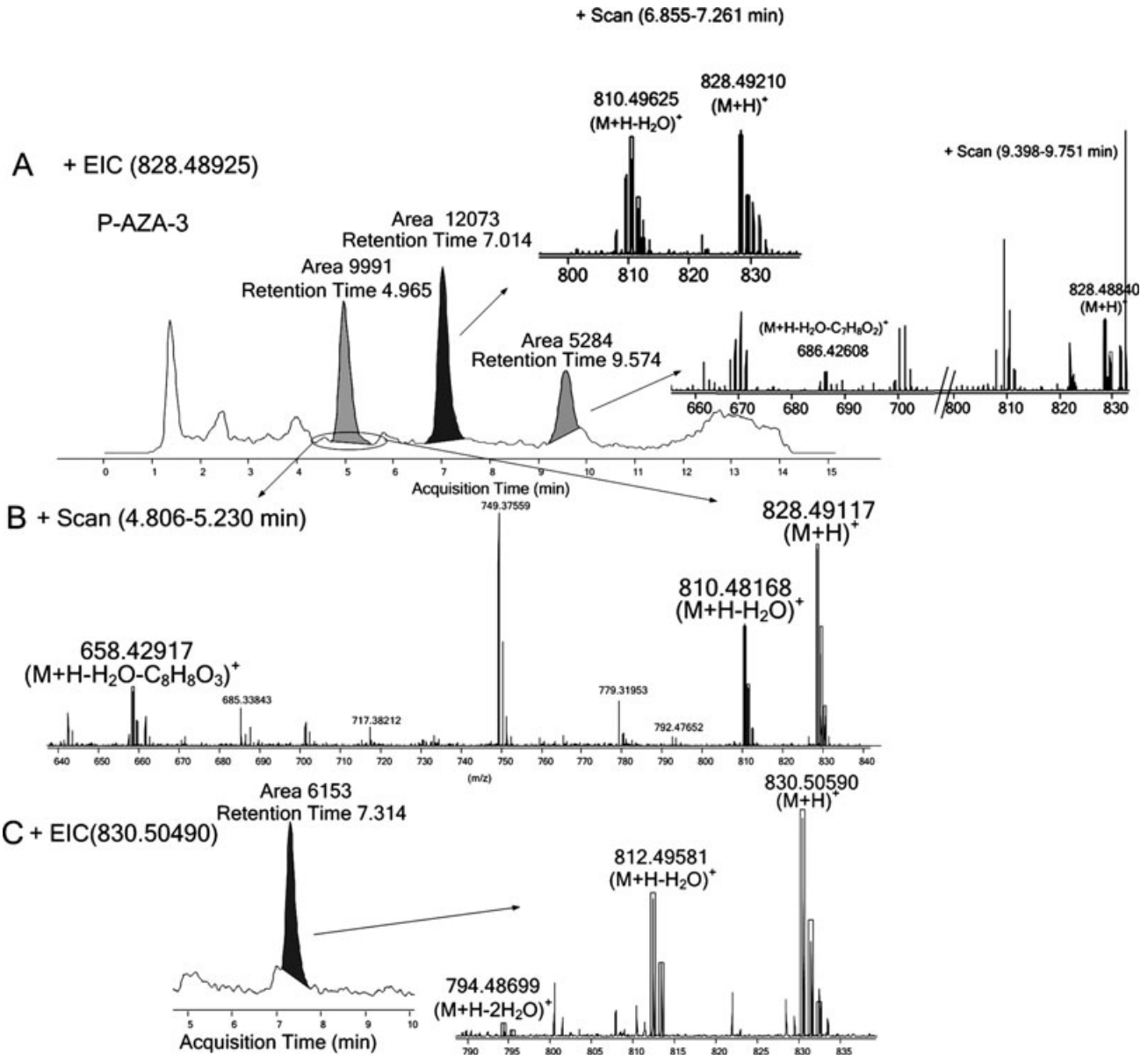

FIG. 10. (A–C) LC/MS-TOF characterization of putative azaspiracid-3 (P-AZA-3) and molecules 828 and 830 from the *Azadinium dexteroporum* culture extract. (A) EIC of compounds having 828.48925 mass, (B) HRMS spectrum of putative AZA-3, (C) EIC and HRMS of molecule 830.

the right side of the theca. Indeed, in *A. caudatum* var. *caudatum*, recently transferred from the genus *Amphidoma* to *Azadinium*, the vp is placed along the right margin of the 1′ plate, while in *A. caudatum* var. *margalefii*, it is in a subapical position, in a notch of the right margin of the Po plate, in contact with the 4′ plate. The two varieties also differ in the shape of the antapical spine. Despite these differences, the small genetic distance and the presence of a morphotype with intermediate morphology of the antapical spine prevented to assign the latter taxa the rank of distinct species (Nézan et al. 2012). The variability of the vp position shown in *A. caudatum* casts some doubts on the use of this character in species delimitation. In the case of *A. dexteroporum*, however, no variation was observed for the vp position within the strain examined or in the single specimen from natural material.

Differently from the other described species, *A. dexteroporum* showed the second intercalary plate concave and collapsed in respect with the other plates. This peculiar feature, initially attributed to a SEM preparation artifact, was evident in all specimens where the plate was observable, and in two different SEM preparations, one obtained few days from the isolation date and the other more than 1 year later. A concave 2a plate may also be present in specimens from Argentinian waters classified as

TABLE 2. Percentage and abundance of the azaspiracids identified in *Azadinium dexteroporum* extract.

Medium	% K	fg · cell^{-1} K	% K/10	fg · cell^{-1} K/10
Putative AZA-3	0.72	0.03	0.44	0.01
Molecule 858	98.80	3.68	97.43	2.22
Molecule 830	0.48	0.02	2.13	0.05

A. cf. *spinosum*, which were responsible for two intense blooms in 1990 and 1991 (Akselman and Negri 2012). Those specimens differ from *A. dexteroporum* for slightly larger dimensions and larger 1a and 3a plates. Unfortunately the most peculiar and clarifying character, i.e., the position of the ventral pore, was not resolved in those specimens.

Several other morphological features distinguish *A. dexteroporum* from the other species of the genus (Table 3). Both *Azadinium poporum* and *Azadinium obesum* lack the antapical spine, and the former has several pyrenoids while the latter does not have a pyrenoid, as compared to the single pyrenoid of *A. dexteroporum*. Like *A. spinosum* and *A. polongum*, *A. dexteroporum* has a small antapical spine, but it is less slender than *A. spinosum* and has smaller 1a and 3a plates, as well as a narrower 1′ plate than those two species. Finally, *A. dexteroporum* is almost three times smaller than the two varieties of *A. caudatum* which, in addition, have a conspicuous antapical horn rather than a small spine. Yet in LM it could be difficult to discriminate *A. dexteroporum* from other small *Azadinium*, and even from other tiny peridinioids. *Azadinium dexteroporum* is the smallest species of the genus but its size range overlaps with almost all other *Azadinium* species, while the presence and the position of the spine and the number of pyrenoids are not always resolved in LM. Besides, the number of pyrenoids cannot be considered a good taxonomic character for dinoflagellate identification, as it may vary over the life cycle and even over the diel cycle (Nagh-Toth et al. 1991, Seo and Fritz 2002).

Morphological identification problems are clearly a hindrance to the assessment of the geographic range of all tiny armored dinoflagellates, especially those within which a few species ≤10 μm are known. These include *Heterocapsa minima* Pomroy, *H. rotundata* (Lohmann) Hansen (Pomroy 1989, Hansen 1995) and the smallest species of the genus *Prorocentrum*, namely *P. nux* Puigserver & Zingone, *P. nanum* Schiller and *P. pusillum* (Schiller) Dodge & Bibby (Puigserver and Zingone 2002). With the exception of *H. rotundata*, which has widely been reported and is probably cosmopolitan (Parke and Dixon 1976, Gil-Rodríguez et al. 2003, Iwataki et al. 2004, Odebrecht 2010), the other small thecate species have rarely been identified after their description. In the case of *Azadinium* species, they have so far been reported from the northeast Atlantic, i.e. the North Sea (Tillmann et al. 2009, 2010, 2011, 2012b) and the Irish coasts (Salas et al. 2011), the

TABLE 3. Morphological features of the described *Azadinium* species.

	A. spinosum	*A. obesum*	*A. poporum*	*A.* cf. *poporum*	*A. polongum*	*A. caudatum* var. *margalefii*	*A. caudatum* var. *caudatum*	*A. dexteroporum*
Length (μm)	12.3–15.7 (n = 73)	13.3–17.7 (n = 36)	11.3–16.3 (n = 48)	10.2–16.1 (n = 100)	10.1–17.4 (n = 107)	25.0–42.1 (n = 59)	35.5–52.5 (n = 31)	7.0–10 (n = 53)
Width (μm)	7.4–10.3 (n = 73)	10.0–14.3 (n = 36)	8.0–11.6 (n = 48)	7.3–11.4 (n = 100)	7.4–13.6 (n = 107)	18.4–30.0 (n = 59)	25.0–36.7 (n = 31)	5.0–8.0 (n = 53)
L/w ratio	1.6	1.3	1.3	1.4	1.3	1.4	1.4	1.4
Antapical spine	Yes	No	No	No	Yes	Yes	Yes	Yes
Pyrenoids	1	0	Several	0–7	0	Not shown	Not shown	1
1″ in touch with 1a	Yes	No	Yes	Yes	Yes	Yes	Yes	Yes
vp position	Left 1′ margin	Left 1′ margin	Left Po end	Left Po end	Left 1′ margin	Right Po margin	Right 1′ margin	Right Po end
1′ plate	Wide	Narrow	Wide	Wide	Wide	Narrow	Narrow	Narrow
1a and 3a	Large	Small	Large	Large	Large	Large	Large	Small
2a	Convex	Convex	Convex	Convex	Convex	Convex	Convex	Concave
3′ plate symmetry	Antero-posterior	Antero-posterior	Antero-posterior	Antero-posterior and lateral	Antero-posterior	Antero-posterior	Antero-posterior	Antero-posterior
Azaspiracids	AZA-1, AZA-2	No	Compound 2	Compound 1	No	Not fully tested	Not tested	Putative AZA-3, 858 and 830 molecules
Distribution	North Sea, Atlantic Ocean	North Sea, Atlantic Ocean	North Sea, Atlantic Ocean	Korea, Pacific Ocean	Shetlands Islands	Mediterranean Sea, Atlantic Ocean	Mediterranean Sea, Atlantic Ocean	Mediterranean Sea
Source	Tillmann et al. 2009,	Tillmann et al. 2010,	Tillmann et al. 2011, Krock et al. 2012,	Potvin et al. 2011, Krock et al. 2012,	Tillmann et al. 2012a,b,	Nézan et al. 2012,	Nézan et al. 2012	This paper

southwest Atlantic Argentinian waters (Akselman and Negri 2012) and the west Pacific Korean waters (Potvin et al. 2011). The large-sized *Azadinium caudatum* is the only species of the genus which has a wider distribution, and it is also reported from the Mediterranean Sea. This report of *A. dexteroporum* in the Tyrrhenian Sea (Mediterranean Sea), along with a finding of the same species in samples from the eastern Adriatic Sea (AZ, unpublished), indicates that also the small *Azadinium* species may be widely distributed and so far overlooked. Indeed, the diversity of these small dinoflagellates should be addressed combining cultivation, SEM and molecular analyses, thus providing the basis for DNA-based identification systems, which will be of great value especially in the case of toxic species.

Azaspiracids. The LC/MS-TOF method used here provided useful information on azaspiracid-like molecules in the *A. dexteroporum* extracts, indicating the presence of compounds having the same atomic composition of AZA-3, AZA-7 and Compound 3. Given the specific characteristics of the instrumentation used, not all the typical fragments so far described for these compounds (Blay et al. 2003, Lehane et al. 2004, Krock et al. 2012) were observed in the material, which deserves further analyses for a definite identification of the azaspiracid-like molecules. Particularly the presence of AZA-7 is dubious, since the molecule has so far been reported only in mussels collected in the natural environment (James et al. 2003, Lehane et al. 2004) and also because of the concomitant finding of fragments belonging to other known compounds.

Along with *A. spinosum*, *A. poporum* and *A.* cf. *poporum*, *A. dexteroporum* is the fourth taxon of the genus that produces azaspiracid-like compounds. This finding enriches the list of potentially harmful species detected along the coasts of the Campania region (Zingone et al. 2006) and attests for the first time the presence of azaspiracids in the Mediterranean Sea. The amount of AZA analogs was lower in the new species as compared to the values of up to 100 fg per cell reported in *Azadinium spinosum*, which, however, varied notably depending on culture conditions (Jauffrais et al. 2012). The amount of toxins was also variable in our two experiments, probably in relation to the sub-optimal physiological condition of the culture in full K medium. Thus, considering this variability and also the well-known intraspecific variability for toxin production in other species, the possible relevance of *A. dexteroporum* to human health issues cannot be ruled out until other strains and/or other conditions are tested.

Concluding remarks. A new *Azadinium* species is reported from Mediterranean waters, where so far only the species *Azadinium caudatum* (syn. *Amphidoma caudata*) was known within this recently erected genus. The new species is clearly distinct from other congeneric species based on molecular data and on a combination of characters, i.e. small size, presence of a small antapical spine, relationships between some plates and shape of the first precingular plate, but it is definitely unique for the configuration of the apical area, the position of the ventral pore and the shape of the second intercalary plate. This first case of an AZA-producing species in the Mediterranean Sea calls for further attempts to bring into culture and to identify tiny dinoflagellates in order to assess the actual frequency and abundance of *Azadinium* species, to uncover other species possibly present in this sea and to evaluate the risk they may represent for human health.

We are grateful to F. Iamunno and R. Graziano (Electron Microscopy Service, SZN) for EM support, to E. Mauriello (Molecular Biology Services, SZN) for DNA sequencing and A. Amato for his precious molecular suggestions. We also wish to thank the Marine Ecology Coastal Areas (MECA) staff for sampling at the LTER-MC station. Two anonymous reviewers are acknowledged for comments that improved the quality of this paper. The study is within the objectives of the EU project ASSEMBLE-FP7-INFRA-2008-227799, which supported IP with a grant. The species described was isolated during a sampling cruise conducted within the project EU-BIODIVERSA BioMarks and is a contribution to the project MIUR-FIRB-BIODIVERSITALIA.

Akselman, R. & Negri, M. 2012. Blooms of *Azadinium* cf. *spinosum* Elbrächter et Tillmann (Dinophyceae) in northern shelf waters of Argentina, Southwestern Atlantic. *Harmful Algae* 19:30–8.

Alvarez, G., Uribe, E., Avalos, P., Marino, C. & Blanco, J. 2010. First identification of azaspiracid and spirolides in *Mesodesma donacium* and *Mulinia edulis* from Northern Chile. *Toxicon* 55:638–41.

Amzil, Z., Sibat, M., Royer, F. & Savar, V. 2008. First report on azaspiracid and yessotoxin groups detection in French shellfish. *Toxicon* 52:39–48.

Andersen, P. & Throndsen, J. 2003. Estimating cell numbers. *In* Hallegraeff, G. M., Anderson, D. M. & Cembella, A. D. [Eds.] *Manual on Harmful Marine Microalgae.* IOC-UNESCO, Paris, pp. 99–129.

Balzano, S., Gourvil, P., Siano, R., Chanoine, M., Marie, D., Lessard, S., Sarno, D. & Vaulot, D. 2012. Diversity of cultured photosynthetic flagellates in the northeast Pacific and Arctic Oceans in summer. *Biogeosciences* 9:4553–71.

Blay, P. S., Brombacher, S. & Volmer, D. A. 2003. Studies on azaspiracid biotoxins. III. Instrumental validation for rapid quantification of AZA 1 in complex biological matrices. *Rapid Commun. Mass Spectrom.* 17:2153–9.

Braña Magdalena, A., Lehane, M., Krys, S., Fernandez, M. L., Furey, A. & James, K. J. 2003. The first identification of azaspiracids in shellfish from France and Spain. *Toxicon* 42:105–8.

Delgado, M. & Fortuño, J. M. 1991. Atlas de fitoplancton del Mar Mediterràneo. *Sci. Mar.* 55(Suppl. 1):1–133.

Doyle, J. J. & Doyle, J. L. 1990. Isolation of plant DNA from fresh tissue. *Focus* 12:13–5.

Edgar, R. C. 2004. MUSCLE: multiple sequence alignment with high accuracy and high throughput. *Nucleic Acids Res.* 32:1792–7.

Furey, A., Moroney, C., Braña Magdalena, A., Fidalgo Saez, M. J., Lehane, M. & James, K. J. 2003. Geographical, temporal, and species variation of the polyether toxins, azaspiracids in shellfish. *Environ. Sci. Technol.* 37:3078–84.

Furey, A., O'Doherty, S., O'Callaghan, K., Lehane, M. & James, K. J. 2010. Azaspiracid poisoning (AZP) toxins in shellfish: toxicological and health considerations. *Toxicon* 56:173–90.

Gil-Rodríguez, M. C., Haroun, R., Ojeda Rodríguez, A., Berecibar Zugasti, E., Domínguez Santana, P. & Herrera Morán, B.

2003. Lista de especies marinas de Canarias (algas, hongos, plantas y animales). *In* Moro, L., Martín, J.L., Garrido, M.J. & Izquierdo, I. [Eds.] *Proctoctista*. Consejería de Política Territorial y Medio Ambiente del Gobierno de Canarias, Las Palmas, pp. 5–30.

Hall, T. A. 1999. BioEdit: a user-friendly biological sequence alignment editor and analysis program for Windows 95/98/NT. *Nucleic Acids Symp. Ser.* 41:95–8.

Hansen, G. 1995. Analysis of the thecal plate pattern in the dinoflagellate *Heterocapsa rotundata* (Lohmann) comb. nov. (= *Katodinium rotundatum* (Lohmann) Loeblich). *Phycologia* 34:166–70.

Iwataki, M., Hansen, G., Sawaguchi, T., Hiroishi, S. & Fukuyo, Y. 2004. Investigations of body scales in twelve *Heterocapsa* species (Peridiniales, Dinophyceae), including a new species *H. pseudotriquetra* sp. nov. *Phycologia* 43:394–403.

James, K. J., Moroney, C., Roden, C., Satake, M., Yasumoto, T., Lehane, M. & Furey, A. 2003. Ubiquitous 'benign' alga emerges as the cause of shellfish contamination responsible for the human toxic syndrome, azaspiracid poisoning. *Toxicon* 41:145–51.

Jauffrais, T., Kilcoyne, J., Séchet, V., Herrenknecht, C., Truquet, P., Hervé, F., Bérard, J. B. et al. 2012. Production and isolation of azaspiracid-1 and -2 from *Azadinium spinosum* culture in pilot scale photobioreactors. *Mar. Drugs* 10:1360–82.

Keller, M. D., Selvin, R. C., Claus, W. & Guillard, R. R. L. 1987. Media for the culture of oceanic ultraphytoplankton. *J. Phycol.* 23:633–8.

Krock, B., Tillmann, U., John, U. & Cembella, A. D. 2009. Characterization of azaspiracids in plankton size-fractions and isolation of an azaspiracid-producing dinoflagellate from the North Sea. *Harmful Algae* 8:254–63.

Krock, B., Tillmann, U., Voß, D., Koch, B. P., Salas, R., Witt, M., Potvin, É. & Jeong, H. J. 2012. New azaspiracids in Amphidomataceae (Dinophyceae). *Toxicon* 60:830–9.

Lehane, M., Fidalgo Saez, M. J., Magdalena, A. B., Ruppen Canas, I., Diaz Sierra, M., Hamilton, B., Furey, A. & James, K. J. 2004. Liquid chromatography-multiple tandem mass spectrometry for the determination of ten azaspiracids, including hydroxyl analogues in shellfish. *J. Chromatogr. A* 1024:63–70.

Margalef, R. 1995. Fitoplancton del NW del Mediteraneo (Mar Catalan) en junio del 1993, y factores que condicionan su producción y distribucción. *Mem. R. Acad. Ciencias Artes Barcelona* 60:3–56.

McMahon, T. & Silke, J. 1996. West coast of Ireland; winter toxicity of unknown aetiology in mussels. *Harmful Algae News* 14:2.

Milne, I., Lindner, D., Bayer, M., Husmeier, D., McGuire, G., Marshall, D. F. & Wright, F. 2008. TOPALi *v*2: a rich graphical interface for evolutionary analyses of multiple alignments on HPC clusters and multi-core desktops. *Bioinformatics* 25:126–7.

Nagh-Toth, F., Peterfi, L. I. & Fodoprataki, L. 1991. Effect of carbon sources on the morphology and structure of *Scenedesmus acutus* Meyen. *Acta Botanica* 37:295–316.

Nézan, E., Tillmann, U., Bilien, G., Boulben, S., Chèze, K., Zentz, F., Salas, R. & Chomérat, N. 2012. Taxonomic revision of the dinoflagellate *Amphidoma caudata*: transfer to the genus *Azadinium* (Dinophyceae) and proposal of two varieties, based on morphological and molecular phylogenetic analyses. *J. Phycol.* 48:925–39.

Odebrecht, C. 2010. Dinophyceae. *In* Forzza, R. C. [Ed.] *Catálogo de plantas e fungos do Brasil*. Vol. 1. Instituto de Pesquisas Jardim Botânico do Rio de Janeiro, Andrea Jakobsson Estúdio, Rio de Janeiro, pp. 366–83.

Orsini, L., Sarno, D., Procaccini, G., Poletti, R., Dahlmann, J. & Montresor, M. 2002. Toxic *Pseudo-nitzschia multistriata* (Bacillariophyceae) from the Gulf of Naples: morphology, toxin analysis and phylogenetic relationships with other *Pseudo-nitzschia* species. *Eur. J. Phycol.* 37:247–57.

Parke, M. & Dixon, P. S. 1976. Checklist of British marine algae. *J. Mar. Biol. Ass. U. K.* 56:527–94.

Pomroy, A. J. 1989. Scanning electron microscopy of *Heterocapsa minima* sp. nov. (Dinophyceae) and its seasonal distribution in the Celtic Sea. *Br. Phycol. J.* 24:131–5.

Posada, D. & Crandall, K. A. 1998. Modeltest: testing the model of DNA substitution. *Bioinformatics* 14:818.

Potvin, E., Jeong, H. J., Kang, N. S., Tillmann, U. & Krock, B. 2011. First report of the photosynthetic dinoflagellate genus *Azadinium* in the Pacific Ocean: morphology and molecular characterization of *Azadinium* cf. *poporum*. *J. Eukaryot. Microbiol.* 59:145–56.

Puigserver, M. & Zingone, A. 2002. *Prorocentrum nux* sp. nov. (Dinophyceae), a small planktonic dinoflagellate from the Gulf of Naples (Mediterranean Sea), and a rediscussion of *P. nanum* and *P. pusillum*. *Phycologia* 41:29–38.

Rampi, L. 1969. Su alcuni elementi fitoplanctonici (Peridinee, Silicococcales ed Heterococcales) rari o nuovi raccolti nelle acque del Mare Ligure. *Natura (Milano)* 60:49–56.

Ribera d'Alcalà, M., Conversano, F., Corato, F., Licandro, P., Mangoni, O., Marino, D., Mazzocchi, M. G. et al. 2004. Seasonal patterns in plankton communities in a pluriannual time series at a coastal Mediterranean site (Gulf of Naples): an attempt to discern recurrences and trends. *Sci. Mar.* 68 (Suppl. 1):65–83.

Salas, R., Tillmann, U., John, U., Kilcoyne, J., Burson, A., Cantwell, C., Hess, P., Thierry, J. & Silke, J. 2011. The role of *Azadinium spinosum* (Dinophyceae) in the production of Azaspiracid Shellfish Poisoning in mussels. *Harmful Algae* 10:774–83.

Seo, K. S. & Fritz, L. 2002. Diel changes in pyrenoid and starch reserves in dinoflagellates. *Phycologia* 41:22–8.

Siano, R., Kooistra, W. H. C. F., Montresor, M. & Zingone, A. 2009. Unarmoured and thin-walled dinoflagellates from the Gulf of Naples, with the description of *Woloszynskia cincta* sp. nov. (Dinophyceae, Suessiales). *Phycologia* 48:44–65.

Taleb, H., Vale, P., Amanhir, R., Benhadouch, A., Sagou, R. & Chaifik, A. 2006. First detection of azaspirazids in mussels in north west Africa. *J. Shellfish Res.* 25:1067–70.

Tamura, K., Peterson, D., Peterson, N., Stecher, G., Nei, M. & Kumar, S. 2011. MEGA5: molecular evolutionary genetics analysis using maximum likelihood, evolutionary distance, and maximum parsimony methods. *Mol. Biol. Evol.* 28:2731–9.

Tillmann, U., Elbrächter, M., John, U. & Krock, B. 2011. A new non-toxic species in the dinoflagellate genus *Azadinium*: *A. poporum* sp. nov. *Eur. J. Phycol.* 46:74–87.

Tillmann, U., Elbrächter, M., John, U., Krock, B. & Cembella, A. 2010. *Azadinium obesum* (Dinophyceae), a new nontoxic species in the genus that can produce azaspiracid toxins. *Phycologia* 49:169–82.

Tillmann, U., Elbrächter, M., Krock, B., John, U. & Cembella, A. 2009. *Azadinium spinosum* gen. et sp. nov. (Dinophyceae) identified as a primary producer of azaspiracid toxins. *Eur. J. Phycol.* 44:63–79.

Tillmann, U., Salas, R., Gottschling, M., Krock, B., O'Driscoll, D. & Elbrächter, M. 2012a. *Amphidoma languida* sp. nov. (Dinophyceae) reveals a close relationship between *Amphidoma* and *Azadinium*. *Protist* 163:701–19.

Tillmann, U., Soehner, S., Nézan, E. & Krock, B. 2012b. First record of the genus *Azadinium* (Dinophyceae) from the Shetland Islands, including the description of *Azadinium polongum* sp. nov. *Harmful Algae* 20:142–55.

Totti, C., Civitarese, G., Acri, F., Barletta, D., Candelari, G., Paschini, E. & Solazzi, A. 2000. Seasonal variability of phytoplankton populations in the middle Adriatic sub-basin. *J. Plankton Res.* 22:1735–56.

Twiner, M. J., Rehmann, N., Hess, P. & Doucette, G. J. 2008. Azaspiracid Shellfish Poisoning: a review on the chemistry, ecology, and toxicology with an emphasis on human health impacts. *Mar. Drugs* 6:39–72.

Ueoka, R., Ito, A., Izumikawa, M., Maeda, S., Takagi, M., Shin-Ya, K., Yoshida, M., van Soest, R. W. M. & Matsunaga, S. 2009. Isolation of azaspiracid-2 from a marine sponge *Echinoclathria* sp. as a potent cytotoxin. *Toxicon* 53:680–4.

Viličić, D., Leder, N., Gržetić, Z. & Jasprica, N. 1995. Microphytoplankton in the Strait of Otranto (eastern Mediterranean). *Mar. Biol.* 123:619–30.

White, T., Bruns, T., Lee, S., Taylor, J., Innis, M., Gelfand, D. & Shinsky, J. 1990. Amplification and direct sequencing of

fungal ribosomal RNA genes for phylogenetics. *In* Innis, M. A., Gelfand, D. H., Sninsky, J. J. & White, T. J. [Eds.] *PCR Protocols: A Guide to Methods and Applications*. Academic Press, New York, pp. 315–22.

Zingone, A., Siano, R., D'Alelio, D. & Sarno, D. 2006. Potentially toxic and harmful microalgae from coastal waters of the Campania region (Tyrrhenian Sea, Mediterranean Sea). *Harmful Algae* 5:321–37.

Supporting Information

Additional Supporting Information may be found in the online version of this article at the publisher's web site:

Table S1. Selected substitution model parameters obtained with Modeltest version 3.7 (Posada and Crandall 1998).

Table S2. MW used to search for azaspiracids in the extract from *Azadinium dexteroporum*.

Table S3. Estimated genetic distances (*P*-values) between species of Amphidomataceae, based on ITS region sequences. Gaps in the alignment were excluded from the comparison.